https://doi.org/10.70882/5td91y76

SCIENCE FORUM (JOURNAL OF PURE AND APPLIED SCIENCES) 26, (5 Special) (2026), 94 - 123

Science Forum (Journal of Pure and Applied Sciences)

Journal Homepage: https://atbuscienceforum.com.ng/index.php/jpas

Photocatalytic Nanomaterials for the Degradation of Organic Pollutants in Wastewater: A Review of Mechanisms, Efficiencies, and Synergistic Approaches

Baydaa Khalaf Jabbar*, Khalida Abaid Samawi, Ekhlas Abd-Alkuder Salman

Department of Chemistry, College of Science, Al-Nahrain University, Baghdad, Iraq.

Abstract

Industrial and municipal wastewater contains high levels of persistent organic pollutants, which represent a severe threat to the environment and water security. Therefore, developing new and innovative treatment technologies that are capable of fully mineralizing these pollutants is needed. Heterogeneous photocatalysis using semiconductor nanomaterials has become one of the most promising advanced oxidation processes to address this problem by providing sustainable, environmentally friendly methods for degrading organic pollutants under solar irradiation. The comprehensive review provides an overview of photocatalytic nanomaterials for the treatment of wastewater, systematically reviewing their mechanism, materials used, and the various means of enhancing their performance through synergism. The review will first discuss the principles of the photocatalytic process using semiconductors with respect to the band structure, charge carrier dynamics and generation of reactive oxygen species (ROS) followed by a critical analysis of the factors affecting the efficiency of photocatalytic reactions. The materials covered will include benchmark metal oxides such as TiO_2, ZnO, WO_3, and Fe_2O_3 and visible-light-active materials such as metal sulfides, bismuth-based compounds, and graphitic carbon nitride. Each photocatalyst will be analyzed for advantages and disadvantages as well as efficiencies as they relate to the degradation of pollutants. Finally, the review will cover the development of synergistic enhancements to address the inherent limitations of photocatalytic materials, which include but are not limited to metal and non-metal doping, Type-II and Z-scheme heterojunctions, carbon-based nanocomposites, and integration with adsorption, Fenton chemistry and photo electrocatalysis. Finally, current challenges impeding practical implementation—scalability, stability, selective degradation, and the need for techno-economic and life cycle assessments—are critically examined, alongside future directions encompassing machine learning-guided material discovery, novel photocatalysts, and process integration. By synthesizing recent literature and identifying key research priorities, this review aims to guide the rational design of efficient, stable, and scalable photocatalytic systems for real-world water purification.

Keywords

Photocatalysis;
Nanomaterials;
Wastewater Treatment;
Organic Pollutants;
Advanced Oxidation Processes;
Heterogeneous Catalysis;
Synergistic Effects.

EISSN: 3156-5190 (Online)
ISSN: 1119-4618 (Print)
JPAS
Faculty of Science, ATBU Bauchi

Corresponding Author: Baydaa Khalaf Jabbar, Department of Chemistry, College of Science, Al-Nahrain University, Baghdad, Iraq.
Email: baydaa.khalaf@nahrainuniv.edu.iq © 2026 Faculty of Science, ATBU Bauchi. All rights reserved

1. Introduction

The growing global water crisis is primarily caused by three major factors: climate change resulting in water shortages; increase in population; and industrial development (Schwarzenbach et al., 2010). The loss of supply as a result of the global water crisis is compounded by the decline in quality of the current water supply as a result of a large volume of recalcitrant organic pollutants being discharged throughout the globe. For example, industrial discharges containing synthetic dyes; agricultural runoff including persistent pesticides; and municipal wastewater comprised of pharmaceuticals, hormones, etc., introduce toxic substances into water sources that are not readily broken down by natural processes (Petrie et al., 2015).

These micropollutants pose serious ecotoxicity risks to both humans and aquatic life even at low concentrations and can lead to immediate and/or long-term health problems if not treated appropriately. Thus, development of comprehensive treatment technologies is critical to mitigating the environmental impact and potential health risks associated with micropollutants. Conventional water treatment technologies have been used to promote public health for over 100 years but do not provide complete mineralization of the newly emerging micropollutants. Techniques such as adsorption, typically using activated carbon, merely transfer the contaminants from the liquid phase to a solid matrix, creating a secondary waste stream that requires further management and disposal (Ali et al., 2012).

Similarly, biological treatment processes, though effective for biodegradable organic matter, are notoriously slow and inefficient against non-biodegradable, complex aromatic structures, and can be inhibited by the very toxic compounds they are meant to eliminate. Physical separation methods like membrane filtration, including reverse osmosis, concentrate pollutants into a reject stream but do not destroy them, leaving the challenge of concentrate disposal unresolved.

Due to these constraints, the use of advanced oxidation treatment methods (AOPs) as a means of destroying organic pollutants completely and non-specifically is highly promising. The basic principle of AOPs is the generation of very reactive and transient species, with the hydroxyl radical (•OH) being particularly important due to its high oxidation potential (2.80 V) (Glaze et al., 1987). The •OH radical is a strong oxidant and will react with most organic compounds at near-diffusion-limited rates, either by abstraction of hydrogen or by addition to an unsaturated bond, which will initiate a series of oxidation reactions that will ultimately lead to the complete mineralisation of the original compound into carbon dioxide and water and inorganic ions.

Of the various AOPs that are available, heterogeneous photocatalysis has attracted considerable interest and is considered to have the greatest potential for being an environmentally sustainable method for purifying water. A heterogeneous photocatalytic process uses semiconductor materials to absorb light (ideally from the sun) to create the necessary electron-hole pairs (free electrons and holes) to be used in producing chemical species known as reactive oxygen species (ROS). Heterogeneous photocatalysis occurs at ambient pressure and temperature and offers considerable economic and environmental advantages compared to energy-intensive processes such as ozonation or UV/H_2O_2 because of the ability to use solar energy as a renewable resource.

Nanomaterials significantly increase the efficiency of photocatalytic systems by virtue of their unique nanoscale properties compared to their larger counterparts. The advantages provided by the nanoscale conversion include a large surface-to-volume ratio that allows for more active sites available for adsorption of pollutants providing a denser quantity of active sites for surface-mediated reactions (Hoffmann, 1995). In addition to increasing the available active sites for reactions, quantum confinement effects cause sizes of nanoparticles smaller than their corresponding Bohr exciton radius to have a tunable bandgap and shift in the respective band edge position giving us the ability to design these materials for a specific light wavelengths and redox potentials. These distinctive physical and

chemical properties of nanostructured photocatalysts such as TiO_2 nanoparticles, ZnO nanorods and g C_3N_4 nanosheets, are able to exhibit greater photocatalytic activity than conventional bulk materials (Kubacka et al., 2012). However, hurdles such as rapid recombination of charge carriers, inefficiencies from non-utilization of broad spectrum of visible light in wide bandgap materials, instability of catalysts, and recovery of used catalysts still hinder commercial application of these systems.

As a result, this paper presents an overview of photocatalytic nanomaterials that are being developed to degrade organic contaminants from the wastewater. The objective of the review is to compile available literature on both an experimental basis and a theoretical basis for photocatalytic activity in order to explain the important photophysical/photochemical phenomena that drive photocatalytic reactions. Subsequently, a large number of photocatalytic materials will be compared with respect to their respective decomposition efficiencies for a variety of different categories of photocatalytic organic contaminants. Lastly, this work will discuss some recent synergistic strategies, such as doped materials, heterojunctions, and carbon composite/copolymer materials, which have been developed to address the limitations of traditional photocatalysts and increase the separation of photogenerated charge carriers, extend the absorption of light into the visible region, and provide technical data for real world applications.

Literature review

The field of photocatalytic nanomaterials for water treatment has rapidly advanced during the past few decades based on a large body of literature and numerous discoveries that have been made along the way. The early stages of this development were anchored by the landmark work of Fujishima and Honda (1972) on the photoelectrochemistry of titanium dioxide (TiO_2), which allowed for an understanding of light-induced charge carrier generation in semiconductors. Carey et al. demonstrated one of the first practical uses of this effect for environmental applications in 1976 by showing that TiO_2 suspensions could photocatalytically degrade polychlorinated biphenyls (PCBs) when exposed to ultraviolet light, stimulating researchers worldwide to continue to optimize TiO_2 as it was considered the "Gold Standard" for photocatalysts due to its exceptional stability, cost-effectiveness, and non-toxicity.

However, TiO_2 also has a fundamental limitation due to its very wide bandgap (approximately 3.2 eV for the anatase phase), which restricts its ability to absorb light to the ultraviolet part of the spectrum represented by < 5% of the irradiance of sunlight. This limitation has resulted in significant research efforts seeking strategies to extend light absorption by TiO_2 into the visible part of the spectrum. One significant breakthrough was the discovery by Asahi et al. (2001) of nitrogen-doped TiO_2, which demonstrated a marked increase in activity when illuminated with visible light and generated significant interest in non-metal dopants as potential modification approaches.

The mechanistic underpinnings of these improvements were further elucidated by studies focusing on charge carrier dynamics; for instance, work by Zhang et al. (1998) employing transient absorption spectroscopy provided critical insights into the competition between interfacial electron transfer and charge recombination, highlighting that the latter is a primary bottleneck limiting quantum efficiency in photocatalytic processes.

At the same time, the effort to find alternate materials that intrinsically absorb visible light was accelerated. Graphitic carbon nitride (g-C_3N_4) is an example of a metal-free, polymeric semiconductor with a medium (approximately 2.7eV) bandgap that was thrust into the limelight for use as an effective photocatalyst by Wang et al., in 2009. The unique layered structure, high thermal and chemical stability, and appropriate band positions for generating reactive oxygen species (ROSs) provided an instant focus for research. After Wang's work on photocatalysis, later works focused on optimizing the textural properties of g-C_3N_4 using hard template

methods to produce a greater specific surface area for photocatalytically degrading dye (Yan et al., 2012). Bismuth-based photocatalysts, like $BiVO_4$ (which has a narrow 2.4 eV bandgap), also attracted attention, primarily due to the systematic evaluation of factors controlling their crystal structure and photocatalytic activity used for O_2 evolution by Kudo et ai., as well as their susceptibility to pollutants, which were determined during this same time period (Kudo et al., 1999).

Similarly, our understanding of the connection between morphology (or structure) and performance improved significantly. Li et al. found that it was possible to control the morphology of $BiVO_4$ crystals such that the exposed crystal facets preferentially facilitate the migration of photogenerated electrons and holes to their corresponding crystal surfaces, thereby promoting the spatial separation of charges in addition to increasing overall reactivity (Li et al., 2013).

Despite the advancements made in creating single-component materials, rapid recombination of charge carriers has continued to hinder attaining high levels of photocatalytic efficiency. This has led to a change of direction in research toward the development of heterostructured nanocomposites in order to achieve synergies that are not achievable by a single material. One example of this type of synergy has been the development of Type-II heterojunctions, consisting of two semiconductors that have staggered band alignments to allow for spatial separation of electrons and holes. An illustrative example of a Type II heterojunction was shown in the work of Amini et al. (2025), who synthesized a TiO_2/g-C_3N_4 core-shell nanostructure and observed greatly improved photodegradation rates of methylene blue under visible light due to efficient transfer of charge from the g-C_3N_4 shell to the TiO_2 core.

A more advanced form of heterojunctions is represented by the Z-scheme, which mimics the natural process of photosynthesis by maintaining the charge carriers with the highest redox potentials. Zhou et al. (2014) demonstrated that they created a direct Z-scheme of g-C_3N_4 and WO_3 by utilizing radical trapping experiments and photoluminescence techniques to provide compelling evidence that the charge transfer mechanism of the Z-scheme was executed by a solid-state Z-scheme pathway, producing a performance greater than either of the single components in the degradation of rhodamine B. The combination of photocatalysts with carbon-based materials has shown to be incredibly beneficial. An example of this can be found in the work done by Zhang et al. (2010), where it was discovered that graphene oxide and TiO_2 can work well together because graphene functions as an exceptional electron transporter and acceptor, thereby significantly reducing charge recombination, reducing charge recombination and enhancing the adsorption of aromatic pollutants due to π-π interactions between them.

In this view, Woan et al. (2009) provided an extensive review placing carbon nanostructures – including carbon nanotubes and fullerenes –in the framework of the major role played by carbon materials as excellent supports and mediators of electron transfer in hybrid photocatalytic systems. The deposition of noble metals onto semiconductor surfaces has been studied for their electron-sinking effect due to the formation of Schottky junctions, as well as for their unique surface plasmon resonance (SPR) effect on photodegrading organic pollutants under visible light. Chen et al.'s (2012) work on Ag/AgX (X = Cl, Br) plasmonic photocatalyst found that the local electromagnetic fields generated by SPR significantly enhance the excitation of charge carriers in adjacent semiconductors, resulting in very high rates of photocatalytic reactions for the breakdown of organic chemicals.

The following table summarizes the key findings from a selection of these pivotal and representative studies, highlighting the materials, target pollutants, reported efficiencies, and the primary focus of each investigation.

Table 1. Summary of Key Photocatalytic Studies and Their Primary Findings.

Author(s) (Year)	Photocatalytic Material(s)	Target Pollutant(s)	Key Finding(s) / Reported Efficiency	Primary Focus of Study
Carey et al. (1976)	TiO_2 suspensions	Polychlorinated biphenyls (PCBs)	Demonstrated first application of TiO_2 photocatalysis for complete dechlorination of PCBs in aqueous solutions.	Foundational application to pollutants
Asahi et al. (2001)	N-doped TiO_2 films and powders	Methylene blue & gaseous acetaldehyde	Reported significant visible-light absorption and enhanced photocatalytic activity due to nitrogen doping.	Non-metal doping for visible light activity
Zhang et al. (1998)	TiO_2 nanoparticles	Chloroform	Used transient absorption spectroscopy to show that electron transfer to O_2 is slow (microseconds), competing with rapid recombination (nanoseconds).	Mechanistic study of charge carrier dynamics
Wang et al. (2009)	g-C_3N_4	Methylene blue	First report on using polymeric g-C_3N_4 for H_2 evolution and dye degradation, highlighting its potential as a metal-free visible-light photocatalyst.	Introduction of g-C_3N_4 to the field
Yan et al. (2012)	Mesoporous g-C_3N_4	Rhodamine B	Achieved enhanced degradation rates by synthesizing g-C_3N_4 with high surface area via a silica-template method.	Morphology optimization
Kudo et al. (1999)	$BiVO_4$	- (O_2 evolution)	Correlated the photocatalytic activity for O_2 evolution with the crystal structure and morphology of $BiVO_4$.	Fundamental study of $BiVO_4$
Li et al. (2013)	$BiVO_4$ with exposed facets	Rhodamine B & water oxidation	Demonstrated that {010} and {110} facets facilitate electron and hole migration respectively, enabling spatial charge separation.	Facet engineering for charge separation
Amini et al. (2025)	TiO_2/g-C_3N_4 core/shell	Methylene blue	The heterojunction showed enhanced visible-light activity due to efficient charge transfer between the two semiconductors.	Type-II heterojunction
Zhou et al. (2014)	g-C_3N_4/WO_3 direct Z-scheme	Rhodamine B	Confirmed a direct Z-scheme mechanism, preserving high redox potential and leading to superior degradation activity.	Z-scheme heterojunction
Zhang et al. (2010)	Graphene/TiO_2 composites	Methylene blue	Graphene acted as an electron acceptor/transporter, reducing recombination and enhancing adsorption via π-π interactions.	Carbon-based nanocomposites
Woan et al. (2009)	Review: Carbon-TiO_2 composites	Various	A comprehensive review summarizing the role of various carbon nanostructures (CNTs, fullerenes, graphene) in enhancing photocatalysis.	Review of carbon nanocomposites

Author(s) (Year)	Photocatalytic Material(s)	Target Pollutant(s)	Key Finding(s) / Reported Efficiency	Primary Focus of Study
Chen et al. (2012)	Ag/AgX (X=Cl, Br) plasmonic	Methyl orange	Surface plasmon resonance of Ag nanoparticles dramatically enhanced visible light absorption and charge carrier generation.	Plasmonic photocatalysis
Liu et al. (2010)	P-doped g-C_3N_4	Rhodamine B & phenol	Phosphorus doping modulated the electronic structure, narrowing the bandgap and improving charge separation and transfer.	Non-metal doping
Di et al. (2015)	$Bi_4O_5Br_2$ ultrathin nanosheets	Ciprofloxacin & tetracycline	Ultrathin structure with surface vacancies promoted charge separation and molecular oxygen activation, leading to high antibiotic degradation.	2D materials and defect engineering
Ndiaye and Akill (2025)	Ag_3PO_4/g-C_3N_4 Z-scheme	Bisphenol A	Constructed a direct Z-scheme heterojunction that exhibited excellent performance and stability for degrading endocrine disruptors.	Z-scheme for emerging pollutants

2. Fundamental Mechanisms of Photocatalysis

The fundamental understanding of photocatalytic mechanisms is essential for the rational design of efficient nanomaterials for wastewater treatment. This section delineates the core principles governing semiconductor photocatalysis, the complex dynamics of charge carriers, the generation of reactive oxygen species (ROS), and the critical factors influencing overall photocatalytic performance, as elucidated by decades of mechanistic investigations.

2.1. The Semiconductor Photocatalysis Principle

The operational framework of heterogeneous photocatalysis is rooted in the unique electronic structure of semiconductor materials, which distinguishes them from metals and insulators.

2.1.1. Band Structure

In semiconductor materials, electrons are grouped together into different bands of energy. A semiconductor has two bands of electron energy, the valence band (VB) and the conduction band (CB). These two bands of electrons are separated by a range of energy where electrons cannot exist, known as a bandgap. Electrons that exist within the VB are tightly bound to atoms (via covalent or ionic bonds) and do not have the energy to move from one atom to another, even at absolute zero. The electrons that exist in the CB of a semiconductor can move from one atom to another freely and, as such, are able to carry electrical current when a sufficient amount of energy is provided to them by an external source of radiation.

The bandgap of a semiconductor is referred to as E_g and is a defining characteristic of a semiconductor. The value of E_g determines the wavelength of radiation required to excite electrons in the conduction band so that they can act as charge carriers; for example, the bandgap (E_g) of anatase (the most studied photocatalyst) TiO_2 is approximately 3.2 eV and corresponds to an absorption threshold in the ultraviolet region (~388 nm) (Linsebigler et al., 1995) for photocatalytic activity. The electronic structure of semiconductors makes it possible to create excitable and charge carrier "excitons" over an extended time period, allowing for controlled use of "excited electrons" for photocatalytic activity; in contrast, conductive metals do not have a bandgap, and therefore cannot be used in this manner.

2.1.2. Photoexcitation and Charge Carrier Generation

The photocatalytic process is initiated when a semiconductor absorbs photons with energy equal to or greater than its bandgap ($h\nu \geq E_g$). This absorption promotes an electron (e^-) from the VB to the CB, leaving behind a positively charged vacancy known as a hole (h^+). This event, termed photoexcitation, generates an electron-hole pair, which constitutes the primary active species in photocatalysis. The number of such pairs generated is directly proportional to the intensity of the incident light and the efficiency of light absorption by the material. As described by Eq. (1), this primary photochemical event transforms the semiconductor into a transient state capable of driving redox chemistry.

$$\text{Photocatalyst} + h\nu \rightarrow \text{Photocatalyst}(e^-_{CB} + h^+_{VB}) \quad (1)$$

2.1.3. Charge Carrier Dynamics

After photoexcitation has occurred, the fate of the created electron-hole pair is determined by several competing kinetic pathways. In order for photocatalysis to work, charge carriers must move to the surface of the nanomaterial to take part in the interfacial redox reactions. However, this desired pathway is continually competing against recombination, where the electron goes back into its original hole and thus loses the energy of absorbed photons as either heat (thermal) or as light (photons). Bulk and surface recombination's are the two places where recombination takes place and represent the principal obstacle to achieving charge carriers' efficiency in photolytic processes, frequently resulting in quantum yields much lower than 1 (Hoffmann et al., 1995). The relative time of each of these events is critical; typically, charge carrier trapping and interfacial transfer take place on femtosecond to picosecond and picosecond to nanosecond time scales, respectively, while recombination may occur on comparable or shorter time scales, rendering suppression of recombination one of the significant hurdles in photocatalysis (Schneider et al., 2014). Figure 1 shows a schematic of these fundamental processes.

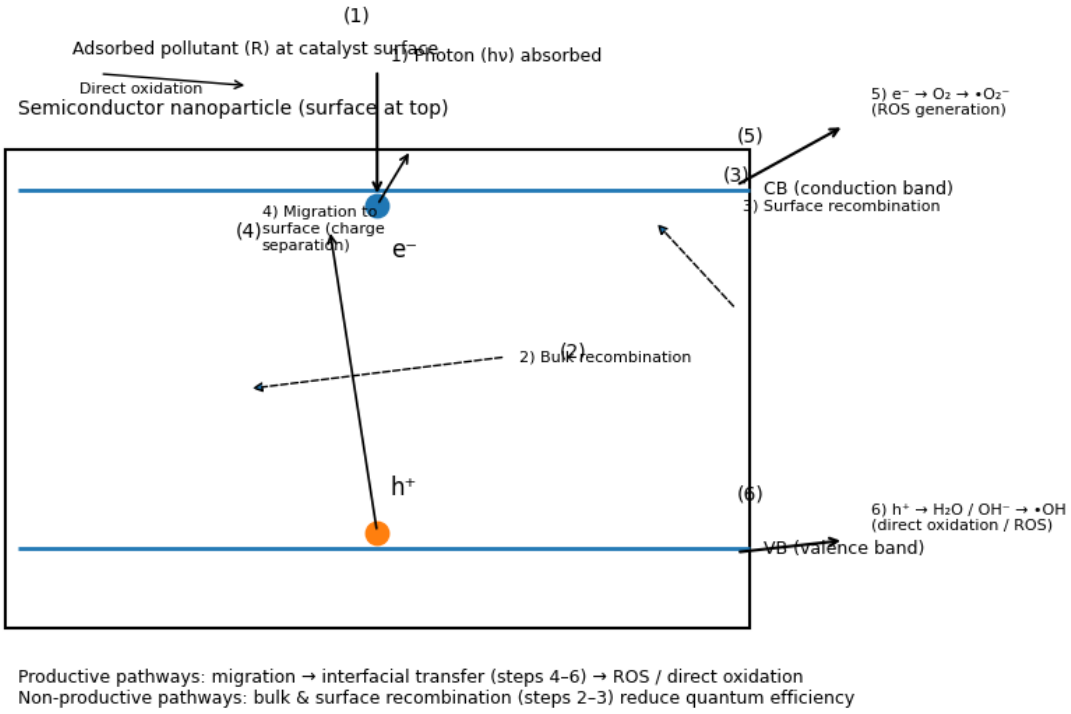

Figure 1. Schematic illustration of the fundamental processes in semiconductor photocatalysis.

(1) Photoexcitation of an electron (e^-) from the valence band (VB) to the conduction band (CB), generating a hole (h^+) in the VB. (2) Bulk recombination of the electron-hole pair. (3) Surface recombination. (4) Migration of charge carriers to the surface. (5) Interfacial electron transfer to an electron acceptor (A). (6) Interfacial hole transfer to an electron donor (D).

Upon absorption of a photon with energy $h\nu \geq E_g$, an electron-hole pair is generated. These charge carriers can either recombine in the bulk or on the surface (non-productive pathways) or migrate to the surface to initiate redox reactions with adsorbed species (productive pathways). The competition between these pathways dictates the overall photocatalytic efficiency.

2.2. Interfacial Charge Transfer and Reactive Oxygen Species (ROS) Generation

Photocatalyst surface sites can trap photoinduced charge carriers after successful migration to the surface, and photoinduced charge carriers can serve as electron donors or acceptors for the adsorbed molecules adsorbed on the photocatalyst surface, such as water and oxygen; and the target organic pollutants (adsorbed on the photocatalyst surface). The electron transfer, between electrons on the photocatalyst surface and adsorbed molecules, leads to the formation of new powerful oxidants called ROS.

2.2.1. Oxidation Reactions

The photogenerated holes in the VB possess a strong oxidation potential. They can participate in two primary pathways. The first is the direct oxidation of an adsorbed organic pollutant (R) by transferring the hole to the molecule, forming a radical cation that subsequently degrades (Eq. 2).

$$h_{VB}^+ + R_{ads} \rightarrow R_{ads}^{+\cdot} \rightarrow \text{Products} \qquad (2)$$

Another pathway for creating ROS in an aqueous environment (and commonly the primary pathway) is that water and surface-associated hydroxyl groups are oxidized (to create the •OH radical) by photoinduced electrons. The •OH radical is one of the most powerful oxidants (oxidizing power of +2.80 volts vs. NHE), and reacts with nearly all organic compounds at near diffusion-limited rates (Glaze et al., 1987). Eqs 3 and 4 show the importance of the reaction of water or hydroxyl radical formed from the oxidation of surface-associated hydroxyl groups during electron transfer to produce the •OH radical.

$$h_{VB}^+ + H_2O_{ads} \rightarrow \cdot OH_{ads} + H^+ \qquad (3)$$
$$h_{VB}^+ + OH_{ads}^- \rightarrow \cdot OH_{ads} \qquad (4)$$

2.2.2. Reduction Reactions

Simultaneously, the photogenerated electrons in the CB act as reducing agents. Their primary role is the reduction of molecular oxygen, which is abundantly present in aerated aqueous solutions. This one-electron transfer yields the superoxide radical ($\cdot O_2^-$), as shown in Eq. (5).

$$e_{CB}^- + O_2 \rightarrow \cdot O_2^- \qquad (5)$$

Superoxide radicals are reactive radicals and may be a reaction participant in degrading contaminants. Additionally, superoxides can react to generate other ROS (Reactive Oxygen Species), for instance (•OOH) (the

hydroperoxyl radical) can be produced when superoxide ($\cdot O_2^-$) is protonated, for example to produce hydrogen peroxide (H_2O_2) (Equations 6). In addition, H_2O_2 can be used as a second electron acceptor as H_2O_2 can then be reduced to form additional ·OH (Equation 7), or can undergo photolysis to yield additional ·OH. Additionally, the energy transferred from an excited state can also create singlet oxygen ($^1O_2$), in addition to an electrophilic ROS.

$$2\cdot O_2^- + 2H^+ \rightarrow H_2O_2 + O_2 \quad (6)$$
$$H_2O_2 + e_{CB}^- \rightarrow \cdot OH + OH^- \quad (7)$$

2.2.3. Direct and Indirect Pathways

It is also important to make a distinction between the two types of oxidation mechanisms that occurs, direct vs indirect. Direct oxidation is the result of the transfer of a photogenerated hole from the photocatalyst to an adsorbed pollutant molecule (Equation 2). This type of pathway is highly relevant for removing pollutants that have been strongly adsorbed to the surface of photocatalysts. Indirect oxidation occurs via the production of ROS generated on the surface of the catalyst, primarily, via ·OH and $\cdot O_2^-$ as the continue to diffuse into solution (liquid) and react with the oxidizing contaminants. The ·OH-mediated pathways are dominant when considering the non-selective mineralization of a wide variety of organic compounds that may be present in trace concentrations (Turchi and Ollis, 1990). The interaction between these two pathways greatly increases the oxidative capabilities of photocatalytic processes. Table 2 summarizes the primary ROS involved in photocatalysis, their formation pathways, and oxidation potentials.

Table 2. Primary Reactive Oxygen Species (ROS) Generated in Photocatalysis.

Reactive Species	Symbol	Formation Reaction(s)	Oxidation Potential (V vs. NHE)
Hydroxyl radical	**·OH**	$h_{VB}^+ + H_2O \rightarrow \cdot OH + H^+;\ h_{VB}^+ + OH^- \rightarrow \cdot OH$	+2.80
Superoxide radical	**$\cdot O_2^-$**	$e_{CB}^- + O_2 \rightarrow \cdot O_2^-$	+1.00 (in DMSO)
Hydrogen peroxide	**H_2O_2**	$2\cdot O_2^- + 2H^+ \rightarrow H_2O_2 + O_2$	+1.78
Singlet oxygen	**$^1O_2$**	Energy transfer from excited states or via $\cdot O_2^-$ reactions	+2.20 (in acetonitrile)

Hydroxyl radicals are the most powerful and non-selective oxidants, primarily generated via hole oxidation of water. Superoxide radicals arise from electron reduction of oxygen and can serve as precursors to other ROS. Oxidation potentials are approximate and can vary with solvent and pH. Adapted from Nosaka and Nosaka (2017).

2.3. Factors Influencing Photocatalytic Efficiency

The overall efficiency of a photocatalytic process is not solely an intrinsic material property but is governed by a complex interplay of catalyst-related features and operational parameters. A substantial body of literature has been dedicated to unraveling these influences.

2.3.1. Catalyst Properties

Physicochemical attributes of nanomaterials are of primary importance: Crystal phase has a large effect on activity, and for example, TiO_2 generally results in photocatalytic activities that differ because of many variables. The anatase phase of TiO_2 is typically much more photo-catalytically active than the rutile phase due to having a way higher fermi level, smaller capacity to provide oxygen for adsorption, and a significantly larger density of surface hydroxyls present (Zhang et al., 2014). Nanoscale morphology guides both the amount of surface area available and which crystal facets will appear most exposed to the environment. For example, one-dimensional (1D) nanorods can create continuous charge paths, while two-dimensional (2D) nanosheets will have much more total surface area than the 1D structure, which may display unique facet-based reactivity - as Li et al. (2013) described with $BiVO_4$ when evaluating the different faceted shapes and how they spatially separated charge carriers (electron and holes).

Generally, the higher the surface area (for example, measured using the BET method), the greater the likelihood there will be active sites for pollutant adsorption and photon absorption. The presence of porosity, especially mesoporosity, helps light scatter within nanomaterials, leading to an overall larger capture of photons and helps reactants diffuse to active sites. Additionally, surface defects (oxygen vacancies) can capture charged carriers storing them until they are ready to be released back to their respective locations, which would lower the probability of recombination while also acting as active sites for reactants to adsorb upon activation (Nowotny et al., 2006). Table 3 summarizes these key catalyst properties and their documented effects on photocatalytic activity, with representative literature examples.

Table 3. Key Catalyst Properties and Their Influence on Photocatalytic Efficiency.

Catalyst Property	Influence on Photocatalysis	Example (Reference)
Crystal Phase	Dictates band structure, surface properties, and charge carrier dynamics.	Anatase TiO_2 shows higher activity for organic oxidation than rutile due to better surface properties and electron mobility (Zhang et al., 2014).
Morphology	Affects surface area, light absorption, and charge transport pathways.	$BiVO_4$ {010} facets accumulate electrons, while {110} facets accumulate holes, enabling spatial charge separation (Li et al., 2013).
Surface Area	Higher area provides more active sites for adsorption and reaction.	Mesoporous g-C_3N_4 with high BET surface area exhibited enhanced rhodamine B degradation compared to bulk g-C_3N_4 (Yan et al., 2012).
Porosity	Mesopores enhance light harvesting via scattering and improve mass transport.	Mesoporous TiO_2 thin films showed increased photocurrent due to improved electrolyte percolation and light scattering (Zukalová et al., 2005).
Surface Defects	Can act as charge carrier traps or adsorption/activation sites.	Oxygen vacancies in TiO_2 can enhance visible-light absorption and act as active sites for O_2 activation (Pan et al., 2013).

The intrinsic properties of photocatalytic nanomaterials, including crystal phase, morphology, surface area, porosity, and defect chemistry, collectively determine their light absorption, charge

separation, and surface reaction capabilities, thereby governing overall efficiency.

2.3.2. Operational Parameters

The nature of photocatalysis is influenced by the physical conditions and the photonic properties of the substance under consideration. The photocatalyst must be at its optimal loading to allow the efficiency of the photocatalysis to be maximized through the absorption of photons; below this optimal loading there will be incomplete absorption of photons, and excess photocatalyst is present to increase scattering and to screen incoming photons from contacting the photocatalyst (Herrmann, 1999). The use of visible-light-active materials is an ongoing quest to harness solar energy more effectively. The pH of the solution influences the surface charge of the catalyst (through its point of zero charge, pH_{PZC}) and the ionization state of the pollutant, thereby affecting adsorption. For instance, TiO_2 has a pH_{PZC} around 6.5; below this pH, its surface is positively charged, favoring the adsorption of anionic pollutants (Chong et al., 2010).

Also, the concentration of the pollutant that is present when photocatalysis begins is crucial to determining the kinetics of the reaction; if the concentration is low, the reaction will typically follow pseudo-first-order kinetics, while at some point as the concentration increases, zero-order kinetics may be reached due to saturation of the active sites. The intensity and wavelength of the light that is impinging upon the photocatalyst are extremely important for this reason; the intensity of the light is directly related to the rate of generation of charge carriers, while the wavelength must equal or exceed the bandgap of the photocatalyst in order for the reaction to occur via photocatalysis.

3. Key Photocatalytic Nanomaterials and Their Efficiencies

Photocatalytic nanomaterials possess an extremely broad spectrum of compositions, structures and electronic characteristics. This section of the report will systematically classify these key photocatalytic materials, from traditional metal oxides to new visible light active semiconductors, critically assess each one based on their key properties, efficiency towards many types of organic pollutants and limitations presented by them, as documented throughout the large volume of existing literature on the subject matter.

3.1. Benchmark Metal Oxide Photocatalysts

Metal oxides represent the most well-studied type of photocatalyst, with titanium dioxide acting as the standard to which all other photocatalysts are compared.

3.1.1. Titanium Dioxide (TiO_2)

Titanium dioxide remains the gold standard in heterogeneous photocatalysis due to its exceptional combination of properties. It exists primarily in three crystalline polymorphs: anatase (tetragonal, $E_g \approx 3.2$eV), rutile (tetragonal, $E_g \approx 3.0$eV), and brookite (orthorhombic, $E_g \approx 3.1$eV), with anatase generally exhibiting the highest photocatalytic activity for organic pollutant degradation (Zhang et al., 2014). The advantages of TiO_2 are manifold: it is photochemically stable, chemically inert in a wide pH range, abundantly available, inexpensive, and non-toxic, making it suitable for environmental applications (Schneider et al., 2014). The properties of TiO_2 have led to a substantial amount of research into its ability to degrade almost all types of organic pollutants. Konstantinou and Albanis (2004) extensively reviewed the photocatalytic degradation of azo dyes on TiO_2 and found that multiple compounds could achieve complete mineralization with UV light.

TiO_2 has also been shown to be effective against many pharmaceutical compounds; for example, Carballa et al. (2004) demonstrated degradation of carbamazepine and diazepam by TiO_2, although complete mineralization usually required a longer exposure period. TiO_2 has a well-documented limitation in that it has a large band gap, which means that TiO_2's photocatalytic activity is limited to the UV region ($\lambda < 387$ nm). Since UV light only accounts for approximately 3 to 5% of solar radiation, this severely limits the effectiveness of solar fuel applications and has led to an increased amount of

research into bandgap engineering and developing visible-light-active alternatives (Pelaez et al., 2012).

3.1.2. Zinc Oxide (ZnO)

Zinc oxide has emerged as a compelling alternative to TiO_2, possessing a similar direct bandgap of approximately 3.2 eV at room temperature. A key advantage of ZnO is its much higher electron mobility (~200-300 $cm^2\ V^{-1}\ s^{-1}$ for bulk ZnO) compared to anatase TiO_2 (~0.1-4.0 $cm^2\ V^{-1}\ s^{-1}$), which facilitates faster transport of photogenerated electrons to the surface and potentially reduces bulk recombination (Mintcheva et al., 2018). This property has translated into high photocatalytic efficiencies in numerous studies. For example, Sapkal et al. (2012) reported that ZnO nanorods achieved 98% degradation of methylene blue within 90 minutes under UV illumination, outperforming commercial TiO_2 (P25) under identical conditions. However, the practical application of ZnO is hindered by a significant drawback: photocorrosion. Upon illumination in aqueous media, ZnO can undergo self-oxidation by its own photogenerated holes, leading to the formation of Zn^{2+} ions in solution and consequent catalyst deactivation (Eq. 8) (Fu et al., 2008).

$$ZnO + 2h^+ \rightarrow Zn^{2+} + \frac{1}{2}O_2 \qquad (8)$$

Research comparing the efficiency of TiO2 and ZnO have produced contradictory conclusions: Sundaram (2004) concluded that TiO2 is superior; however, other studies have found that ZnO is actually superior. Results are often influenced by the type of pollutant, type of light used, and how the catalyst is constructed. However, photocorrosion is a major limitation to consider, which is why developing ways to passivate the surface of ZnO or create a heterojunction to remove positive holes before they can cause damage to the ZnO structure is necessary.

3.1.3. Other Metal Oxides

Beyond TiO_2 and ZnO, several other metal oxides have been investigated for their photocatalytic potential, often targeting visible-light activity. Tungsten trioxide (WO_3) possesses a relatively narrow bandgap of 2.4-2.8 eV, enabling absorption of visible light up to approximately 520 nm. It exhibits good stability in acidic conditions and has a deep valence band, endowing it with strong oxidation power for holes. However, its conduction band position is often too positive (~+0.5 V vs. NHE) to effectively reduce molecular oxygen to superoxide ($E°(O_2/•O_2^-)$ = -0.33 V vs. NHE), limiting electron utilization and necessitating an electron acceptor or a coupled system (Bamwenda & Arakawa, 2001).

Hematite (a-Fe_2O_3) is another attractive visible-light-active material with a bandgap of 1.9-2.2 eV, absorbing light up to ~650 nm. Its abundance, low cost, and high stability are significant advantages. Zinc oxide's (ZnO) photocatalytic ability is highly restricted due to very low hole diffusion (2-4 nm), fast charge recombination and a conduction band that is poorly positioned for O_2 reduction (Moattari and Mahinroosta, 2025).

Copper oxide (CuO and Cu_2O) has narrow bandgap (1.2–1.9 eV) and absorbs visible light; however, these materials are subject to photocorrosion (like ZnO) and fast charge recombination (Tran et al., 2014). Table 4 shows important properties of these benchmark metal oxide photocatalysts.

Table 4. Key Properties and Characteristics of Benchmark Metal Oxide Photocatalysts.

Photocatalyst	Bandgap (eV)	Light Absorption	Advantages	Limitations	Representative Reference
TiO_2 (Anatase)	3.2	UV (λ < 388 nm)	Stable, cheap, non-toxic, high activity	Wide bandgap, UV-only active	Schneider et al. (2014)
ZnO	3.2	UV (λ < 388 nm)	High electron mobility, similar activity to TiO_2	Photocorrosion in aqueous media	Sapkal et al. (2012)
WO_3	2.4 - 2.8	Visible (λ < 520 nm)	Visible light active, stable in acid, deep VB	Poor CB position for O_2 reduction	Bamwenda & Arakawa (2001)
α-Fe_2O_3	1.9 - 2.2	Visible (λ < 650 nm)	Abundant, cheap, narrow bandgap	Poor charge separation, short hole diffusion length	Moattari & Mahinroosta (2025)
CuO	1.2 - 1.9	Visible (λ > 650 nm)	Very narrow bandgap, visible/NIR absorption	Photocorrosion, rapid recombination	Tran et al. (2014)

Benchmark metal oxide photocatalysts offer a range of bandgaps and properties. While TiO_2 and ZnO are highly active UV photocatalysts, others like WO_3 and Fe_2O_3 absorb visible light but suffer from poor charge carrier dynamics or unsuitable band positions.

3.2. Visible-Light-Active Photocatalysts

The quest to harness the abundant visible region of the solar spectrum has driven intense research into photocatalysts with narrower bandgaps.

3.2.1. Metal Sulfides

Compared to oxides, certain metals and their metal sulphides have a smaller band gap. This is due to the fact that the bandedge of both are S-3p orbitals, which are the valence states for metal sulphides, that means S-3p orbitals tend to start at an energy level higher than that of O-2p orbitals, which are the valence states for oxides. For example, cadmium sulphide (CdS) has a bulk bandgap, which means its conduction band (valence band) bottom edge, of approximately 2.4 eV, which gives it the ability to absorb photons with wavelengths up to approximately 520 nm. The negative potential of the conduction band edge of CdS is sufficient to permit both O_2 reduction and proton reduction.

Consequently, CdS has attracted a lot of research attention as a degradation agent for organic dyes and other environmental pollutants using only visible light. For example, it has been reported that CdS nanowires were able to degrade > 90% of rhodamine B in 60 minutes using exclusively visible light (Mondal & Saha, 2012). Although CdS performs well in degrading organics, it has a significant disadvantage of having a high degree of photocorrosion. In CdS, the photogenerated holes oxidizing the sulphide ions (S^{2-}) in the crystal lattice to form elemental sulphur (S^0) causes the dissolution/deactivation of the catalyst (Eq. 9) (Huang et al. 2013).

$$CdS + 2h^+ \rightarrow Cd^{2+} + S \qquad (9)$$

In order to address this issue, some of the ways that have been studied are pairing CdS with an additional material that will protect the photocatalyst (e.g., TiO_2, ZnS), or employing chemical scavengers for holes. Bao et al. (2008) provided evidence that when CdS is coated with ZnS, the coating enhances the stability of the coated material due to the enhanced capability of the ZnS to transfer holes away from the CdS core. Molybdenum disulfide (MoS_2) (which is a layered type of transition metal dichalcogenide) has received attention as a co-catalyst rather than

as a primary photocatalyst because of the conductivity characteristics of MoS_2 in its metallic 1T phase and the activity at its edge sites.

The bulk form of MoS_2 has an indirect bandgap of 1.3 eV, and its monolayer structure has a direct bandgap of 1.9 eV, but the photocatalytic activity of MoS_2 by itself is relatively low, so the majority of its use has been as a component of heterojunctions (Li et al., 2011). Zinc sulfide (ZnS) is a semiconductor with a wide bandgap (3.7 eV) and is often referenced as a representative sulfide because of its stability and its use in solid solutions with CdS to modify cadmium's bandgap and improve its stability.

3.2.2. Bismuth-Based Photocatalysts

Bismuth-based semiconductors have emerged as a prominent class of visible-light-driven photocatalysts, distinguished by their unique electronic structures and layered crystal architectures. The hybridization of Bi 6s and O 2p orbitals in these materials creates a highly dispersed valence band, which facilitates the mobility of photogenerated holes and contributes to their excellent visible light absorption (Kudo et al., 1999). Bismuth vanadate ($BiVO_4$), with a bandgap of approximately 2.4 eV, has been extensively studied for water oxidation and pollutant degradation.

Its photocatalytic activity is highly dependent on crystal phase and morphology; the monoclinic scheelite phase is the most active. For example, Li et al. (2013) demonstrated that by controlling the exposure of specific crystal facets, photogenerated electrons and holes could be spatially separated on {010} and {110} facets of $BiVO_4$, respectively, leading to enhanced degradation of rhodamine B. Bismuth tungstate (Bi_2WO_6) is another important member, possessing a layered Aurivillius structure with a bandgap of 2.7–2.8 eV.

It has shown excellent activity for the degradation of various dyes and pharmaceuticals under visible light. Zhang et al. (2007) reported that Bi_2WO_6 nanoplates could completely mineralize rhodamine B within 60 minutes under visible light, attributing the high activity to the efficient charge separation within its layered structure. The bismuth oxyhalides, BiOX (X = Cl, Br, I), form a family of materials with layered structures characterized by $[Bi_2O_2]$ slabs interleaved with double halogen atom layers. This structure creates an internal electric field perpendicular to the layers, which is highly conducive to the separation of photogenerated electrons and holes. Their bandgaps are tunable by varying the halogen atom, ranging from ~3.4 eV for BiOCl (UV-active) to ~1.8 eV for BiOI (visible-active). Di et al. (2015) demonstrated that ultrathin $Bi_4O_5Br_2$ nanosheets, a member of this family, exhibited exceptional activity for ciprofloxacin degradation under visible light, attributed to surface vacancies and efficient charge separation.

3.2.3. Graphitic Carbon Nitride (g-C_3N_4)

Graphitic carbon nitride (g-C_3N_4) has revolutionized the field as a metal-free, polymeric semiconductor photocatalyst. Typically synthesized by thermal polymerization of nitrogen-rich precursors such as melamine, urea, or dicyandiamide, g-C_3N_4 possesses a moderate bandgap of approximately 2.7 eV, corresponding to an absorption edge around 460 nm in the visible region (Wang et al., 2009). Its structure consists of tri-s-triazine units connected via tertiary amines, forming a two-dimensional layered structure analogous to graphite. The advantages of g-C_3N_4 are compelling: it is composed of earth-abundant elements, exhibits high thermal and chemical stability (resisting oxidation in air up to 600 °C), and has a suitable conduction band position (-1.3 V vs. NHE) for O_2 reduction and a valence band position (+1.4 V vs. NHE) for water oxidation to •OH.

Since its introduction to photocatalysis by Wang et al. (2009) for hydrogen production, it has been widely applied for pollutant degradation. For instance, Yan et al. (2012) showed that mesoporous g-C_3N_4 achieved 98% degradation of rhodamine B under visible light in 180 minutes, with the enhanced surface area playing a crucial role. Despite these merits, bulk g-C_3N_4 suffers from a high charge recombination rate, moderate specific surface area, and limited absorption beyond 460 nm. Consequently, a vast body of literature has been dedicated to modifying g-C_3N_4 through strategies such as nanostructuring (e.g., nanosheets, nanotubes), elemental doping (e.g., S, P, O), and heterojunction construction to overcome these limitations (Liu et al., 2010; Lan et al., 2016). Table 5 summarizes the properties and efficiencies of key visible-light-active photocatalysts.

Table 5. Key Visible-Light-Active Photocatalysts and Their Reported Efficiencies.

Photocatalyst	Bandgap (eV)	Light Range (nm)	Pollutant	Efficiency / Rate Constant (k)	Key Reference
CdS nanowires	2.4	< 520	Rhodamine B	90% in 60 min	Mondal and Saha (2012)
$BiVO_4$ (faceted)	2.4	< 520	Rhodamine B	Enhanced degradation vs. un-faceted	Li et al. (2013)
Bi_2WO_6 nanoplates	2.8	< 440	Rhodamine B	100% in 60 min	Zhang et al. (2007)
$Bi_4O_5Br_2$ nanosheets	~2.8	< 440	Ciprofloxacin	High degradation, superior to bulk	Di et al. (2015)
Mesoporous g-C_3N_4	2.7	< 460	Rhodamine B	98% in 180 min (k = 0.023 min^{-1})	Yan et al. (2012)
P-doped g-C_3N_4	~2.6	< 480	Rhodamine B	3.2× higher rate than bulk g-C_3N_4	Liu et al. (2010)

Visible-light-active photocatalysts, including metal sulfides, bismuth-based compounds, and g-C_3N_4, demonstrate significant activity for pollutant degradation under visible light. Their efficiencies are often enhanced through morphological control, facet engineering, or elemental doping.

3.3. Comparative Analysis of Efficiencies

To provide a holistic view of the field, Table 6 presents a comparative summary of selected photocatalytic nanomaterials. This table synthesizes data from a range of studies, highlighting key material properties and their reported degradation efficiencies for various model pollutants. It is important to note that direct comparison across different studies is challenging due to variations in experimental conditions (e.g., light source intensity, reactor geometry, pollutant concentration). However, such a compilation serves to illustrate the diverse landscape of photocatalytic performance and provides a useful reference for material selection and benchmarking.

Table 6. Comparative Summary of Photocatalytic Nanomaterials and Their Efficiencies.

Material Class	Specific Material	Bandgap (eV)	Light Absorption Range	Specific Surface Area (m^2/g)	Model Pollutant	Degradation Efficiency / Rate Constant (k)	Key Reference
Metal Oxide	TiO_2 (P25)	3.2	UV	~50	Methylene Blue	100% in 60 min (UV)	Konstantinou & Albanis (2004)
Metal Oxide	ZnO Nanorods	3.2	UV	~20-30	Methylene Blue	98% in 90 min (UV)	Sapkal et al. (2012)
Metal Oxide	WO_3	2.6	Visible	~10-15	Rhodamine B	Moderate activity, requires e^- acceptor	Bamwenda & Arakawa (2001)
Metal Sulfide	CdS Nanowires	2.4	Visible	~50-70	Rhodamine B	>90% in 60 min (Vis)	Mondal and Saha (2012)
Bismuth-Based	$BiVO_4$ (monoclinic)	2.4	Visible	~5-10	Rhodamine B	High activity, facet-dependent	Li et al. (2013)
Bismuth-Based	Bi_2WO_6 Nanoplates	2.8	Visible	~30-50	Rhodamine B	100% in 60 min (Vis)	Zhang et al. (2007)
Bismuth-Based	$Bi_4O_5Br_2$ Nanosheets	~2.8	Visible	~100	Ciprofloxacin	Superior to bulk, high activity	Di et al. (2015)
Polymeric	g-C_3N_4 (bulk)	2.7	Visible	~10	Rhodamine B	Moderate (k ~0.01 min^{-1})	Yan et al. (2012)
Modified Polymer	g-C_3N_4 (mesoporous)	2.7	Visible	~150	Rhodamine B	Enhanced (k ~0.023 min^{-1})	Yan et al. (2012)

Material Class	Specific Material	Bandgap (eV)	Light Absorption Range	Specific Surface Area (m^2/g)	Model Pollutant	Degradation Efficiency / Rate Constant (k)	Key Reference
Modified Polymer	P-doped g-C_3N_4	~2.6	Visible	~50	Rhodamine B	3.2× bulk rate	Liu et al. (2010)

This comparative table illustrates the diversity in properties and reported efficiencies of key photocatalytic nanomaterials. Variations in specific surface area, bandgap, and morphology directly influence the observed degradation rates for model pollutants. Note that direct cross-study comparisons should be made with caution due to differing experimental conditions.

4. Synergistic Approaches for Enhanced Photocatalysis

The continuing difficulties resulting from rapid charge carrier recombination and insufficient absorption of visible light by single component photocatalysts have resulted in the need for new and sophisticated methodologies developed to improve photocatalytic performance. This section critically evaluates several of the synergistic systems that have been created to address these fundamental challenges and thereby improve the performance of photocatalysts to the point where they can be used for practical application. The development of these strategies makes use of the different synergetic effects that result from the combination of multiple components (i.e., doped; heterojunctions built from mixed semiconductors; and integration with carbonaceous materials), which demonstrate enhanced performance then if the individual components were to operate alone.

4.1. Doping with Metals and Non-Metals

Doping, which is defined as an intentional addition of foreign atoms into the crystal lattice of a semiconductor, is one of the most commonly studied approaches to alter the electrical and/or optical properties of photocatalysts.

4.1.1. Metal Doping

The incorporation of metal ions into semiconductor lattices introduces impurity energy levels within the bandgap, fundamentally altering the material's optoelectronic properties. Transition metal ions (e.g., Fe, Cu, Cr, Mn) can serve as electron or hole traps, temporarily immobilizing charge carriers and thereby suppressing electron-hole recombination (Choi et al., 2002). For instance, doping TiO_2 with Fe^{3+} ions introduce Fe 3d states within the TiO_2 bandgap, which can act as shallow traps for both electrons and holes, extending their lifetime and enhancing photocatalytic activity for pollutant degradation. Zhu et al. (2006) demonstrated that Fe-doped TiO_2 nanoparticles exhibited significantly higher activity for 4-nitrophenol degradation compared to undoped TiO_2, attributing the enhancement to improved charge separation.

The operation of noble metal nanoparticles (e.g. Au, Ag, and Pt) that are placed onto semiconductor surfaces occurs through two independently-existing synergistic mechanisms. First, the disparities between their work function values will result in a Schottky junction being formed at the metal-semiconductor interface. This junction produces an internal electric field to move photogenerated electrons from the conduction band of the semiconductor to the metal nanoparticle, where they are physically separated from their associated holes, leading to significant suppression of recombination (Subramanian et al., 2004). Second, when Au and Ag nanoparticles interact with incident light of specific wavelengths, their conduction electrons will collectively oscillate, and will produce electromagnetic fields of great strength through a process called surface plasmon resonance (SPR). These intense local electric fields may greatly increase the excitation of charge carriers within the adjacent semiconductor and allow for hot electrons to be injected directly into the conduction band of the semiconductor from the plasmonic metal (Linic et al., 2011). This was demonstrated by Chen et al. (2012) for Ag/AgCl plasmonic photocatalysts, where SPR excitation of the Ag nanoparticles resulted in extremely high activity for the degradation of methyl orange when exposed to visible light. For g-C_3N_4, significant exploration has been done on the effects of metal doping with a variety of metals such as K, Fe, and Pt. Zhang et al. (2010) reported that Fe-doped g-C_3N_4 exhibited enhanced visible light absorption and improved photocatalytic activity for rhodamine B degradation due to the formation of mid-gap states that facilitated charge transfer.

4.1.2. Non-Metal Doping

Nitrogen, sulfur, carbon, and phosphorus non-metal doping have shown to enhance visible light absorption in wide-bandgap photocatalysts. Unlike metal-doped systems, non-metals such as these typically replace oxygen or nitrogen atoms within these lattices, creating new energy levels within or near the edge of the valence band. Asahi et al.'s (2001) landmark study on N-doped TiO_2 demonstrated that N 2p and O 2p levels interact to effectively raise the edge of the valence band, decrease the band gap, and maintain the reducing potential of the conduction band. This landmark study spurred extensive research on visible-

light-active N-TiO_2 for degrading environmental pollutants. For example, Sathish et al. (2007) synthesized N-doped TiO_2 with varying amounts of added nitrogen, finding a direct relationship between the nitrogen loading and the amount of visible light absorbed by the N-TiO_2, where the optimum sample achieved 96% degradation of methylene blue under visible light.

In addition to TiO2, g-C3N4 has also been doped with nonmetals extensively. For example, Liu et al. (2010) demonstrated that doped phosphorus on g-C3N4 can be accomplished by means of thermal co-polymerization of melamine and hexachlorocyclotriphosphazene resulting in P substituting for C in the tri-s-triazine ring thus altering the electronic structure from 2.69 eV to 2.62 eV thus providing improved charge separation/transfer and resulting a 3.2 times increase of the degradation of the rhodamine B. Similarly, Liu et al. (2010) have shown that using trithiocyanuric acid as a precursor to dope sulfur into g-C3N4 results in S being substituted into the framework thereby extending the absorption of visible light and improving photocatalyctic activity. Table 7 provides the details of several case studies utilizing metal and non-metal doping strategies.

Table 7. Representative Studies on Metal and Non-Metal Doping for Enhanced Photocatalysis.

Doping Type	Dopant Element	Host Material	Key Finding	Enhancement Mechanism	Reference
Metal	Fe^{3+}	TiO_2	Enhanced 4-nitrophenol degradation	Charge carrier trapping, reduced recombination	Zhu et al. (2006)
Metal (Noble)	Au	TiO_2	Enhanced photocatalytic activity	Schottky junction for electron sink, SPR effect	Subramanian et al. (2004)
Metal (Plasmonic)	Ag	Ag/AgCl	Exceptional visible-light activity for methyl orange	SPR-enhanced excitation and hot electron injection	Chen et al. (2012)
Metal	Fe	$g\text{-}C_3N_4$	Enhanced rhodamine B degradation	Mid-gap states for improved charge transfer	Zhang et al. (2010)
Non-Metal	N	TiO_2	Visible-light activity for methylene blue and acetaldehyde	Bandgap narrowing by mixing N 2p with O 2p states	Asahi et al. (2001)
Non-Metal	P	$g\text{-}C_3N_4$	3.2-fold enhancement for rhodamine B degradation	Electronic structure modulation, improved charge separation	Liu et al. (2010)
Non-Metal	S	$g\text{-}C_3N_4$	Enhanced visible light absorption and activity	Bandgap narrowing, extended π-conjugation	Liu et al. (2010)

Doping with metals and non-metals introduces impurity states or modulates the band structure of host photocatalysts, leading to enhanced visible light absorption, reduced charge recombination, and improved photocatalytic activity for pollutant degradation.

4.2. Heterojunction Construction

The construction of heterojunctions by coupling two or more semiconductors with appropriate band alignments represents one of the most powerful strategies for achieving spatial separation of photogenerated charge carriers, thereby mitigating recombination and enhancing photocatalytic efficiency.

4.2.1. Type-II Heterojunctions

When two semiconductors display staggered band alignments, type-II heterojunctions are created between them, with both the conduction band and valence band of one semiconductor being lower than those of the other. When both materials are excited by light (photoexcitation), electrons that are

created in the higher conduction band of semiconductor A move to the lower conduction band of semiconductor B, and electron "holes" created in the lower valence band of semiconductor B also flow to the higher valence band of semiconductor A.

By separating electrons and holes spatially across the interface of the two semiconductors, recombination events will be severely limited, resulting in much longer charge carrier lifetimes (Wang et al., 2014). An example of this would be the TiO_2/CdS heterojunction. With its much wider bandgap, TiO_2 can give a stable framework, and it has a deep valence band, so electrons will have a strong driving force for oxidation via to the TiO_2 conduction band. On the other hand, because CdS has a narrower bandgap, it will effectively act as a visible light sensitizer. In fact, the photoexcited electrons in the CdS conduction band at −0.5 V vs. NHE can efficiently transfer to the TiO_2 conduction band at −0.3 V vs. NHE, while holes generated in the CdS valence band remain there for effective charge separation.

Bessekhouad et al. (2004) confirmed that TiO_2/CdS heterojunctions were significantly more effective than either pure TiO_2 or CdS for photodegradation of malic acid when tested under visible light. Another widely studied system is ZnO/g-C_3N_4. Wang et al. (2011) fabricated ZnO nanorods decorated with g-C_3N_4 nanoparticles and observed enhanced photodegradation of methylene blue under UV-visible light, attributed to efficient electron transfer from the CB of g-C_3N_4 to the CB of ZnO and hole transfer in the opposite direction. Figure 2A provides a schematic illustration of the charge transfer mechanism in a Type-II heterojunction.

4.2.2. Z-Scheme Heterojunctions

The Type II Heterojunction (TJ) effectively separates the charge carriers (electrons and holes) created during an excited state through the energy level (band) configuration of the respective TJ materials. However, because the TJ separates these carriers, it has the disadvantage of actually lowering the redox potential of the electrons and holes since they can migrate to lower energy bands. The Z-Scheme Heterojunction (ZJ), designed based on the fundamental principles of the natural photosynthesis process of green plants, is therefore a remedy to this problem, since this configuration retains the charge carriers (electrons and holes) with the highest redox potential. In a ZJ configuration, two semiconductors are coupled by either direct connection (ie, interface) or indirectly (ie, conductive mediator). In the case of an interface connection, the electrons in the lower conduction band (CB) semiconductor (lower work function) that have been photoexcited recombine with the holes of the higher valence band (VB) semiconductor (higher work function), thereby leaving the electrons in the higher CB and the holes in the lower VB and therefore having very strong reduction and oxidation potential, respectively (Zhou et al., 2014).

Z-scheme systems are broadly classified into two types: traditional liquid-phase Z-schemes, which employ a reversible redox mediator (e.g., IO_3^-/I^-, Fe^{3+}/Fe^{2+}) in solution to facilitate charge transfer, and all-solid-state Z-schemes, where a solid conductive material (e.g., graphene, Au) or direct contact enables charge recombination. The direct Z-scheme, without a mediator, has garnered significant attention due to its simplicity and efficiency. Zhou et al. (2014) constructed a direct Z-scheme g-C_3N_4/WO_3 heterojunction and, through radical trapping experiments and photoluminescence studies, confirmed that the charge transfer mechanism followed a solid-state Z-scheme path.

The resulting composite exhibited superior activity for rhodamine B degradation compared to either single component or a physical mixture, demonstrating the power of the Z-scheme approach. Another prominent example is the $BiVO_4$/g-C_3N_4 direct Z-scheme system, which combines the strong oxidation power of $BiVO_4$ holes with the strong reduction power of g-C_3N_4 electrons. Li et al. (2016) reported that $BiVO_4$/g-C_3N_4 composites showed significantly enhanced activity for ciprofloxacin degradation under visible light, attributed to efficient charge separation and preservation of high redox potentials. Figure 2B provides a schematic illustration of the charge transfer mechanism in a direct Z-scheme heterojunction.

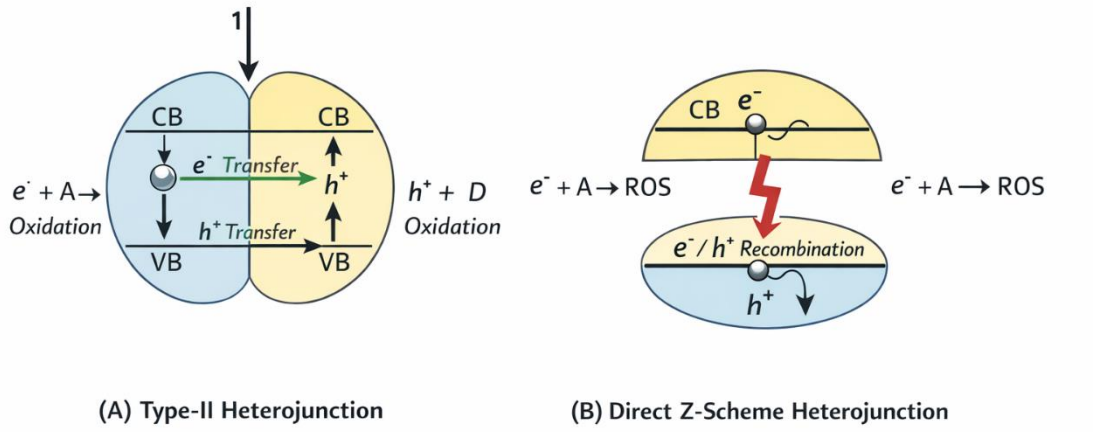

Figure 2. Schematic comparison of charge transfer mechanisms in (A) Type-II and (B) direct Z-scheme heterojunctions.

Electrons and holes migrate to the lower CB and higher VB, respectively at the Type II heterojunction (A), allowing for spatial separation but losing redox potentials. Conversely, at the direct Z-scheme heterojunction (B), electrons from the semiconductor B lower CB recombine with holes from the semiconductor A upper VB, maintaining the electrons with high reductive potentials at the A CB and the holes with high oxidative potential (VB of semiconductor B).

Type II heterojunctions allow for separation of the spatial charge but at the expense of the reduction potential. Direct Z-scheme heterojunctions, which are modeled after natural photosynthesis, allow for the recombination of lower energy charge carriers across the heterointerface, maintaining charge carriers with the greatest reduction and oxidation potentials.

4.3. Carbon-Based Nanocomposites

Carbonaceous nanomaterials, with their exceptional electrical conductivity, high surface area, and unique electronic properties, have emerged as ideal components for constructing high-performance photocatalytic nanocomposites.

4.3.1. Graphene and its Derivatives

The two-dimensional sheet of sp^2-hybridised carbon – graphene – and its derivatives, graphene oxide (GO) and reduced graphene oxide (rGO), have been thoroughly evaluated and integrated with photocatalysts. Graphene's predominant role in these composites is to aid as a superior electron acceptor and transporter. Due to their high work functions and exceptional electron mobilities, photogenerated electrons found within the semiconductor's conduction band (CB) transfer rapidly to the graphene sheet and subsequently leave the semiconductor-graphene interface, effectively suppressing charge recombination (Zhang et al., 2010).

The theorised large specific surface area of graphene of ~2,600 m^2/g also creates many possible adsorption sites for organic pollutants, concentrating them at or near the photocatalytic active sites and enhancing their degradation kinetics through π-π interactions with other aromatic pollutants. Zhang et al. (2010) demonstrated this synergistic mechanism in composites of P25 and graphene by showing their increasing photocatalytic activity for the degradation of methylene blue compared to P25 alone, suggesting that graphene was both an electron acceptor and an adsorption enhancer.

4.3.2. Carbon Nanotubes

Carbon nanotubes (CNTs), whether single-walled or multi-walled, behave like graphene and act as electron conductive wires that enable quick charge transfer off of the surface of a photocatalyst. Because they are one-dimensional, they create pathways for electron transport in a directed way. A systematic review was done by Woan and colleagues (2009) on the use of CNTs in composites made with TiO_2 and has shown that these materials utilize CNTs to accept photogenerated electrons from TiO_2 so as to decrease the rate of recombination. Additionally, depending on the presence of carbonaceous materials, CNTs can also sensitise TiO_2 to visible light. CNTs also improve pollutant adsorption due to their high surface area and hydrophobicity.

4.3.3. Other Carbon Materials

Recently, carbon dots (CDs) have received significant attention due to their potential as multipurpose materials for use in photocatalytic systems. CD's (zero-dimensional 0D) include graphene quantum dots (GQDs) and carbon quantum dots (CQDs). GQDs & CQDs exhibit superior characteristics than traditional photocatalysts (widely considered as having broad band gap), in terms of their unique ability (photoluminescent behaviour) to absorb lower energy (visible or near infrared (NIR)) and emit higher energy (ultraviolet (UV) or visible) in an up-conversion manner, thereby broadening the wavelengths of light that can be used by traditional photocatalysts (Li et al., 2010). In addition, GQDs and CQDs function as an electron mediator and reservoir through accepting & shuttling electrons which creates a pathway for charge separation. For example, Di et al., (2017) demonstrated that modified (with CQDs) BiOCl ultrathin nanosheets displayed greater capacity for the activation of molecular oxygen and broad-band photocatalytic activity for the degradation of ciprofloxacin using the synergistic properties of CDs. The relevant examples of carbon-based nanocomposite systems can be found in Table 8.

Table 8. Representative Carbon-Based Nanocomposites for Enhanced Photocatalysis.

Carbon Material	Photocatalyst	Key Finding	Enhancement Mechanism	Reference
Graphene (rGO)	TiO_2 (P25)	Enhanced methylene blue degradation	Electron acceptor/transporter, enhanced adsorption via π-π interactions	Zhang et al. (2010)
Carbon Nanotubes	TiO_2	Comprehensive review of enhancement mechanisms	Electron transfer, visible light sensitization, enhanced adsorption	Woan et al. (2009)
Carbon Dots	BiOCl	Enhanced ciprofloxacin degradation, broad-spectrum activity	Up-conversion, electron mediation, enhanced O_2 activation	Di et al. (2017)
Graphene	g-C_3N_4	Enhanced rhodamine B degradation	Improved charge separation, extended light absorption	Valadez-Renteria et al. (2023)
Carbon Nanotubes	CdS	Enhanced visible-light activity and stability	Efficient electron transfer, reduced photocorrosion	Kim et al. (2011)

Carbon-based nanomaterials, including graphene, carbon nanotubes, and carbon dots, enhance photocatalytic performance by accepting and transporting photogenerated electrons, suppressing recombination, and, in the case of carbon dots, extending light absorption through up-conversion.

4.4. Other Synergistic Integrations

Beyond doping, heterojunctions, and carbon composites, photocatalysis can be synergistically integrated with other physical and chemical processes to achieve enhanced pollutant degradation.

4.4.1. Photocatalysis Coupled with Adsorption

The coupling of photocatalysts to high surface area adsorbents leads to a synergistic effect whereby the adsorbent concentrates pollutants in proximity to photocatalytic active sites, allowing for their easy degradation afterwards. This method is especially useful for treating pollutants at low concentrations where the transport of mass to the surface of the catalyst can be rate limiting. Common adsorbent supports include zeolites, clays (such as montmorillonite), and activated carbon. For example; zeolite supported TiO_2 has been shown to have increased photocatalytic activity from adsorption of pollutants onto the zeolite and also because of the creation of highly reactive species trapped inside the pore structure of the zeolite (Reddy et al., 2009).

The close association between the adsorbent and photocatalyst provides an excellent opportunity for adsorbed pollutants to be exposure to photogenerated reactive oxygen species (ROS) which will lead to physical concentration and chemical destruction of these pollutants.

4.4.2. Photo-Fenton Processes

The Fenton process, involving the reaction of Fe^{2+} with H_2O_2 to generate •OH (Eq. 10), is a powerful AOP in its own right. However, its efficiency is limited by the slow regeneration of Fe^{2+} from Fe^{3+} and the consumption of iron sludge. Combining photocatalysis with the Fenton process, termed the photo-Fenton process, overcomes these limitations. In this system, light (UV or visible) irradiates the Fe^{3+}/H_2O_2 mixture, promoting the photoreduction of Fe^{3+} back to Fe^{2+} (Eq. 11), thereby sustaining the Fenton cycle and enhancing •OH production (Pignatello et al., 2006).

$$Fe^{2+} + H_2O_2 \rightarrow Fe^{3+} + \bullet OH + OH^- \quad (10)$$

$$Fe^{3+} + H_2O + h\nu \rightarrow Fe^{2+} + \bullet OH + H^+ \quad (11)$$

When a solid photocatalyst is also present, the system becomes a heterogeneous photo-Fenton process, where photogenerated electrons from the semiconductor can further contribute to Fe^{3+} reduction and H_2O_2 activation, creating a highly synergistic environment for ROS generation. For instance, Fe_2O_3/g-C_3N_4 composites have been explored as photo-Fenton catalysts, demonstrating enhanced degradation of organic pollutants through the combined effects of photocatalytic charge separation and Fenton chemistry (Liu et al., 2010).

4.4.3. Photoelectrocatalysis

The field of photoelectrocatalysis (PEC) combines photocatalysis with electrochemistry. The primary difference from photocatalysis is that PEC utilizes an applied external bias potential to enhance the efficiency of the process. To achieve this, a photocatalyst layer is deposited onto a conductive substrate such as fluorine-doped tin oxide (FTO) and an applied bias creates an electric field within the semiconductor film; this electric field drives the transport of photogenerated electrons towards their back contacts and counter electrode while concurrently transporting holes to the surface where they participate in oxidation reactions. The application of an external driving force enables an additional means of separating charge carriers, greatly reducing the likelihood of recombination and enhancing the availability of holes for oxidizing pollutants (Bessegato et al., 2015).

Overall, PEC systems exhibit much higher degradation efficiencies for all types of pollutants when compared to photocatalytic systems alone, particularly for the difficult-to-oxidize pollutant class. For example, TiO_2 nanotube arrays used as photoanodes in PEC configurations have been studied extensively as a means to degrade many organic pollutants and the use of an applied bias ensures that photogenerated electrons are efficiently collected and retained, thus ensuring that there is a maximum number of holes available for reaction at the surface (Liu et al., 2011).

5. Current Challenges and Future Perspectives

There are a number of significant challenges that stand in the way of transferring discoveries regarding nanoscale materials for photocatalytic purposes from the laboratory into actual wastewater treatment systems. These challenges fall across three broad disciplines: material science, chemical engineering, and environmental economics. This section discusses these challenges and offers some recommendations for potential future research directions that will help to move the field closer to developing sustainable, large-scale technologies for treating wastewater using photocatalytic nanomaterials. To address these issues, researchers will need to shift their thinking about how photocatalytic technologies will operate under realistic conditions, rather than under the idealised laboratory conditions in which they were originally developed.

5.1. Scalability and Reactor Design

Most photocatalytic experimentations/experiments and studies take place in laboratories with small reactors, standardized light sources, and model pollutants in ideal and controlled conditions. Once the experimental process has been demonstrated,

the next step is to scale the application of photocatalysis into pilot and industrial scales. This move creates/develops engineering complexity, and many individuals tasked with scaling-up projects underestimate the many engineering challenges involved in the transition from laboratory- to industrial-scale photocatalyst application. One of the key challenges within this transition of photocatalysis is the immobilization of the photocatalyst. Slurry reactors using suspended nanoparticles have a very high effective surface area and demonstrate very high mass transfer rates; however, they require a post-treatment/separation step (to recover the photocatalyst) that requires a substantial amount of energy and can be very expensive (Kubacka et al., 2012).

Conversely, using fixed supports such as glass beads, optical fibres, and/or membranes to immobilize the photocatalyst removes the need for a post-treatment process; however, it creates new engineering challenges (e.g., less effective surface area for photoreaction, mass transfer limitations, and potential detachment of the photocatalyst with time).

The second major obstacle to overcome is that light penetration in photoreactors is less than totally effective. The Lambert Beer law states that the intensity of light diminishes exponentially as it penetrates through an absorptive and scattering medium, such as a slurries contain a significant amount of catalyst, which can inhibit the light from reaching beyond the first few millimetres of the reactor, leaving a majority of the reactor in complete darkness and underutilised (Hambourger et al., 2009). Of course, this requires new and innovative photoreactor geometries to accommodate and optimise light distribution, such as thin film reactors, annular reactors or optical fibre reactors that channel light to the depths of the reaction media.

Additionally, the need for transition from batch to continuous flow operation (which is crucial for the industrial treatment of wastewater) must be analysed in terms of residence time distribution, hydrodynamics and maintenance of uniform catalyst distribution or stable immobilised films. Loeb et al. (2018) have presented a comprehensive discussion of the technical obstacles to using photocatalytic methods for water treatment and have pointed out that advances in reactor engineering need to keep pace with advances in material technology (i.e.,photocatalysts) so as to eliminate the gap between laboratory success and commercial viability.

5.2. Stability and Reusability

The use of photocatalytic nanomaterials in practical applications is dependent on their long-term operational stability under continuous illumination and after coming into contact with a variety of complex wastewater matrices. Unfortunately, many photocatalysts that have good photocatalytic activity can also be significantly unstable, as described in more detail in previous sections, for example, CdS and other metal sulfides can be severely affected by photocorrosion, as the photogenerated holes oxidize the lattice-bound sulfide ions resulting in the dissolution of the catalyst and leaching of toxic metal ions (Huang et al., 2013).

Even though ZnO is an efficient photocatalyst, in an aqueous environment (especially at extreme pH values), it can also be subject to similar photocorrosion. On the other hand, TiO2, which is widely used and chemically stable, can be deactivated as a result of fouling caused by the adsorption of non-degradable intermediates and other inorganic materials contained within the actual wastewater, thus blocking the active sites of the catalyst and progressively deactivating it.

The enhancement of the stability of a photocatalyst is therefore an important goal. With regard to materials that suffer from photochemical degradation (such as CdS), surface behaviour (passivation) through a shell to protect against the extraction of charge carriers (holes) from the core crystal lattice (for example, coating CdS with ZnS or TiO_2) has been successfully used (Bao et al., 2008). Likewise, to overcome materials that are subject to

fouling, it may be necessary to develop self-cleaning surfaces or to implement periodic cleaning procedures.

The determination of the functional reusability of photocatalysts is currently performed by conducting multiple cycles of photocatalytic degradation, providing valuable data on the rates of catalyst degradation and the frequency of catalyst regeneration. Nonetheless, there are currently very few studies (as discussed in Spasiano et al., 2015) conducted over an extended period (hundreds of hours) and under practical conditions to establish valid lifetime expectations and replacement costs of photocatalyst materials.

5.3. Selective Degradation versus Total Mineralization

There is a notable difference between a photocatalytic wastewater treatment method designed to mineralize organic pollutants into carbon dioxide, water, and inorganic ions compared to a process that degrades organic compounds into less hazardous or potentially recoverable products (Lu 2013). The original goal of mineralizing organic pollutants to the extent they disappear completely takes so long that it produces greater amounts of oxidants than would be desired from a standpoint of energy usage (the longer the reaction takes, the more oxidants will be produced).

Therefore, in some situations where one wishes to oxidize valuable organic compounds or where energy is a limiting factor of oxidation processes, a selective oxidation of these organic compounds into either less hazardous or recoverable products may be an avenue worth considering. For example, oxidizing biomass-derived compounds or oxidative intermediates produced in pharmaceutical manufacturing through a selective photocatalytic oxidation reaction could produce valuable organic compounds and/or meet the principles associated with the circular economy and waste recovery and resource recovery.

While pursuing a selective oxidation of organic compounds can provide value and/or environmentally meaningful outcomes, it will require an understanding of the reaction mechanisms that take place during photocatalytic oxidation, as well as the ability to convert the reactive/oxidative species present in the reaction to favorably influence the pathway by which the organic pollutant is being destructively oxidized. Specific strategies for imparting or enhancing selectivity may include modifying the surface properties of the photocatalyst (e.g., depositing functional groups onto the photocatalyst surface or creating molecularly imprinted sites) to increase the likelihood that a specific organic pollutant will be selectively oxidized; tuning the band structure of the photocatalyst; or using a photocatalyst that primarily generates specific ROS.

The challenge lies in balancing selectivity with activity and ensuring that partially oxidized by-products are not more toxic or persistent than the parent compounds. Future research should therefore explore the potential for photocatalytic processes to be not merely destructive but also productive, converting waste streams into resources where feasible.

5.4. Techno-Economic Analysis and Life Cycle Assessment

For decades, scientists have successfully studied photocatalytic nanomaterials, yet there are few studies comparing their economic viability or environmental impact against other established treatment technologies. Quantitative analysis of the tech-econ (or techno-economic analysis, TEA) will help quantify all the costs associated with the production of photocatalysts, construction of reactors, and energy consumption (e.g., for artificial lighting) and replacing or regenerating catalysts in comparison to traditional treatment methods (i.e., activated carbon adsorption, biological treatment, and advanced oxidation processes: ozone & UV/H2O2; see Ioannou-Ttofa et al., 2016) will involve capital/operating costs & the value of the treated water; and the avoided costs due to environmental degradation.

In addition to Technology Evaluation and Assessment (TEA), Life Cycle Assessment (LCA) also provides an integrated perspective on the environmental impacts

from the extraction of the raw materials used to create the catalyst right through to the disposal of the spent material. LCAs are also able to provide an alternative or less visible environmental trade-off; for example, a highly efficient photocatalytic material that uses rare or toxic materials may have an extremely high environmental impact from its manufacture and thus, offset any benefits from its improved performance (Walser et al., 2011). TJ's TEA and LCA assessments will therefore provide a means to inform and ensure that photocatalytic technologies are not only scientifically sound and economically viable but also sustainable, thus requiring additional work to integrate TEA and LCA with performance data to make a realistic assessment of the potential feasibility of photocatalytic wastewater treatment technologies.

5.5. Future Directions

Addressing the challenges outlined above requires a multifaceted, forward-looking research agenda that embraces new methodologies, materials, and system integrations. The use of machine learning (ML) and artificial intelligence has the potential to transform both the identification of new photocatalytic materials and the optimization of the performance of previously discovered photocatalytic materials. By utilizing large data sets that contain physical and chemical properties of photocatalytic materials, new photocatalytic materials can be identified by predicting their characteristics through use of ML models.

In addition, ML can help scientists and researchers find characteristics related to the activity of photocatalytic materials, guide experimental activities away from trial-and-error, and provide research scientists with directions on where to look when searching for new photocatalytic materials (Steiman et al., 2020). Use of ML will enable the investigation of large sample spaces associated with a very large numbers of compositions of materials used in doped systems and composites at a very rapid rate, potentially identifying materials with very high performance and stability faster than any method currently used.

Research into novel photocatalytic materials that possess superior performance characteristics and long-term stability is ongoing. An alternative to photocatalytic materials currently being researched includes the use of metal-organic framework (MOF)-based materials. With their extremely large surface areas, tunable pore structures, and potential to act as hosts for photocatalytic materials, MOFs represent an opportunity to create new photocatalytic materials with superior performance properties that are not currently available. In addition, many MOFs exhibit semiconductor-like behavior when they are exposed to light, and their well-defined structures will enable researchers to more easily correlate the performance of these materials with their molecular structures (Wang & Wang, 2015). Another example of a potential source for photocatalytic materials is halide perovskites. Recent years have produced vast amounts of positive attention on the use of halide perovskite materials (e.g., $CH_3NH_3PbI_3$) to create photovoltaic devices due to their impressive optoelectronic performance, and researchers are now considering using these materials as photocatalytic substrates. Nonetheless, the challenges associated with the water solubility of perovskite materials will need to be addressed to ensure that lead-free, water-stable materials are available (Brenner et al., 2016).

The design of laboratory experiments needs to change considerably. Instead of testing the breakdown of single compound model contaminants in pure water, it needs to test the treatment of actual wastewater blends. Actual wastewaters are a blend of multiple compounds and contain various types of organic and inorganic materials as well as natural organic matter that can scavenge ROS, compete for active sites and foul catalysts (Loos et al., 2013). It is imperative that studies validating a new material's potential for practical applications should be conducted on a true wastewater matrix or on at least a synthetic mixture that mimics the complexity of real wastewater matrices.

It is an ambitious but critical goal to use more of the solar spectrum for photocatalysis. This includes harnessing the near infrared (NIR) area, which

accounts for almost half of the sun's energy output. This will involve creating new photocatalysts with extremely narrow band gaps or photocatalysts that can up-convert NIR photons into visible light or UV, which can then be photochemically active on a conventional photocatalyst. Lanthanide-doped up-conversion nanoparticles are an emerging area of research, particularly in combination with semiconductors such as TiO_2, for the purpose of enhancing photocatalysis using the NIR region (Xu et al., 2016). However, the efficiencies of such systems remain at a low level, and significant advancements must occur to create sufficient material improvements.

Finally, integrating photocatalysis with other sustainable technologies could create hybrid systems with enhanced overall performance and energy efficiency. For example, coupling photocatalytic reactors with microbial fuel cells (MFCs) could enable simultaneous wastewater treatment and electricity generation, where the MFC treats biodegradable components while photocatalysis addresses recalcitrant pollutants, potentially using the electricity generated by the MFC to power the photocatalytic process (Li et al., 2015). Such integrative approaches, while complex, embody the systems-thinking necessary to develop truly sustainable water treatment solutions for the future. Table 9 summarizes these challenges and future directions.

Table 9. Summary of Current Challenges and Future Perspectives in Photocatalytic Wastewater Treatment.

Aspect	Current Challenges	Future Perspectives and Strategies
Scalability	Catalyst recovery, light penetration, continuous flow operation	Innovative reactor design (thin-film, optical fiber), effective immobilization techniques
Stability	Photocorrosion (sulfides, ZnO), fouling, long-term deactivation	Surface passivation, protective coatings, development of inherently stable materials
Treatment Goal	Trade-off between selective degradation and complete mineralization	Valorization of by-products, selective oxidation for resource recovery
Economic/Environmental Assessment	Lack of TEA and LCA studies for realistic scenarios	Integrate TEA and LCA with experimental research to assess viability
Material Discovery	Slow, trial-and-error experimentation	Machine learning-guided discovery and optimization
Novel Materials	Need for stable, efficient, visible-light-active materials	Exploration of MOFs, water-stable perovskites, and other advanced materials
Experimental Realism	Over-reliance on single-pollutant model systems	Focus on real wastewater matrices and complex pollutant mixtures
Light Utilization	Limited absorption of solar spectrum (UV/Vis only)	Harness NIR light via up-conversion or narrow-bandgap semiconductors
Process Integration	Photocatalysis as a standalone process	Integration with MFCs, membrane filtration, or other sustainable technologies

The translation of photocatalytic technologies from laboratory to market requires addressing critical challenges in scalability, stability, and economic viability. Future research must embrace advanced computational tools, novel materials, realistic experimental conditions, and system-level integration to overcome these hurdles.

6. Conclusion

This review demonstrates the excellent promise photocatalytic nanomaterials exhibit in solving the worldwide environmental issue of organic pollutants found in water. Their application could lead to the complete mineralization of contaminants that are extremely persistent through the use of reactive oxygen species created from ambient conditions. Key topics that have been reviewed are key aspects of photocatalysis such as the physical mechanics that govern photocatalysis; Band structure, Charge carrier dynamics and interfacial charge transfer to determine photocatalytic efficiency. Materials that have been examined include key photocatalytic materials that have been developed since the beginning of photocatalysis.

They have moved from the benchmark metal oxides such as Tio_2 that is still considered to be the gold standard of photocatalytic materials due to its stability and non-toxicity to a wide variety of visible light activated systems such as Bi-Based compounds, Metal sulfides and metal free polymers such as carbon nitride. A key conclusion is that no one material has all the attributes needed for effective commercial applications; each material has its limitations (i.e Wide Bandgap, Photocorrosion susceptibility and rapid charge recombination).

Therefore, the review has also highlighted that the use of synergistic strategies (i.e Elemental Doping, Heterojunction construction, (Type II and Z-Scheme) and/or incorporation with Carbonaceous materials) will be effective for improving and enhancing photocatalytic efficiency by improving light absorption, suppressing recombination losses and improving the utilization of charge carriers. The translation of these promising nanomaterials from laboratory-scale successes to viable, real-world wastewater treatment technologies requires continued interdisciplinary research that integrates materials innovation with chemical engineering, environmental science, and economic analysis, ultimately bridging the gap between fundamental understanding and practical implementation.

References:

Asahi, R., Morikawa, T., Ohwaki, T., Aoki, K., & Taga, Y. (2001). Visible-light photocatalysis in nitrogen-doped titanium oxides. *Science*, *293*(5528), 269–271.

Bamwenda, G. R., & Arakawa, H. (2001). The visible light induced photocatalytic activity of tungsten trioxide powders. *Applied Catalysis A: General*, *210*(1–2), 181–191.

Bao, N., Shen, L., Takata, T., & Domen, K. (2008). Self-templated synthesis of nanoporous CdS nanostructures for highly efficient photocatalytic hydrogen production under visible light. *Chemistry of Materials*, *20*(1), 110–117.

Bessegato, G. G., Guaraldo, T. T., de Brito, J. F., Brugnera, M. F., & Zanoni, M. V. B. (2015). Achievements and trends in photoelectrocatalysis: from environmental to energy applications. *Electrocatalysis*, *6*(5), 415–441.

Bessekhouad, Y., Robert, D., & Weber, J. V. (2004). Bi_2S_3/TiO_2 and CdS/TiO_2 heterojunctions as an available configuration for photocatalytic degradation of organic pollutant. *Journal of Photochemistry and Photobiology A: Chemistry*, *163*(3), 569–580.

Brenner, T. M., Egger, D. A., Kronik, L., Hodes, G., & Cahen, D. (2016). Hybrid organic–inorganic perovskites: low-cost semiconductors with intriguing charge-transport properties. *Nature Reviews Materials*, *1*(1), 1–16.

Carballa, M., Omil, F., Lema, J. M., Llompart, M., García-Jares, C., Rodríguez, I., ... & Ternes, T. (2004). Behavior of pharmaceuticals, cosmetics and hormones in a sewage treatment plant. *Water Research*, *38*(12), 2918–2926.

Carey, J. H., Lawrence, J., & Tosine, H. M. (1976). Photodechlorination of PCB's in the presence of titanium dioxide in aqueous suspensions. *Bulletin*

of Environmental Contamination and Toxicology, *16*(6), 697–701.

Chen, D., Li, T., Chen, Q., Gao, J., Fan, B., Li, J., ... & Gao, L. (2012). Hierarchically plasmonic photocatalysts of Ag/AgCl nanocrystals coupled with single-crystalline WO_3 nanoplates. *Nanoscale*, *4*(17), 5431–5439.

Choi, W., Termin, A., & Hoffmann, M. R. (1994). The role of metal ion dopants in quantum-sized TiO_2: correlation between photoreactivity and charge carrier recombination dynamics. *The Journal of Physical Chemistry*, *98*(51), 13669–13679.

Chong, M. N., Jin, B., Chow, C. W., & Saint, C. (2010). Recent developments in photocatalytic water treatment technology: a review. *Water Research*, *44*(10), 2997–3027.

Di, J., Xia, J., Ji, M., Wang, B., Yin, S., Zhang, Q., ... & Li, H. (2015). Carbon quantum dots modified BiOCl ultrathin nanosheets with enhanced molecular oxygen activation ability for broad spectrum photocatalytic properties and mechanism insight. *ACS Applied Materials & Interfaces*, *7*(36), 20111–20123.

Fu, H., Xu, T., Zhu, S., & Zhu, Y. (2008). Photocorrosion inhibition and enhancement of photocatalytic activity for ZnO via hybridization with C_{60}. *Environmental Science & Technology*, *42*(21), 8064–8069.

Fujishima, A., & Honda, K. (1972). Electrochemical photolysis of water at a semiconductor electrode. *Nature*, *238*(5358), 37–38.

Glaze, W. H., Kang, J. W., & Chapin, D. H. (1987). The chemistry of water treatment processes involving ozone, hydrogen peroxide and ultraviolet radiation. *Ozone: Science & Engineering*, *9*(4), 335–352.

Hambourger, M., Moore, G. F., Kramer, D. M., Gust, D., Moore, A. L., & Moore, T. A. (2009). Biology and technology for photochemical fuel production. *Chemical Society Reviews*, *38*(1), 25–35.

Herrmann, J. M. (1999). Heterogeneous photocatalysis: fundamentals and applications to the removal of various types of aqueous pollutants. *Catalysis Today*, *53*(1), 115–129.

Hoffmann, M. R., Martin, S. T., Choi, W., & Bahnemann, D. W. (1995). Environmental applications of semiconductor photocatalysis. *Chemical Reviews*, *95*(1), 69–96.

Huang, L., Wang, X., Yang, J., Liu, G., Han, J., & Li, C. (2013). Dual cocatalysts loaded type I CdS/ZnS core/shell nanocrystals as effective and stable photocatalysts for H_2 evolution. *The Journal of Physical Chemistry C*, *117*(22), 11584–11591.

Ioannou-Ttofa, L., Foteinis, S., Chatzisymeon, E., & Fatta-Kassinos, D. (2016). The environmental footprint of a membrane bioreactor treatment process through Life Cycle Analysis. *Science of the Total Environment*, *568*, 306–318.

Kim, Y. K., & Park, H. (2011). Light-harvesting multi-walled carbon nanotubes and CdS hybrids: application to photocatalytic hydrogen production from water. *Energy & Environmental Science*, *4*(3), 685–694.

Konstantinou, I. K., & Albanis, T. A. (2004). TiO_2-assisted photocatalytic degradation of azo dyes in aqueous solution: kinetic and mechanistic investigations: a review. *Applied Catalysis B: Environmental*, *49*(1), 1–14.

Kubacka, A., Fernandez-Garcia, M., & Colon, G. (2012). Advanced nanoarchitectures for solar photocatalytic applications. *Chemical Reviews*, *112*(3), 1555–1614.

Kudo, A., Omori, K., & Kato, H. (1999). A novel aqueous process for preparation of crystal form-

controlled and highly crystalline $BiVO_4$ powder from layered vanadates at room temperature and its photocatalytic and photophysical properties. *Journal of the American Chemical Society*, *121*(49), 11459–11467.

Lan, Z. A., Zhang, G., & Wang, X. (2016). A facile synthesis of Br-modified g-C_3N_4 semiconductors for photoredox water splitting. *Applied Catalysis B: Environmental*, *192*, 116–125.

Li, H., He, X., Kang, Z., Huang, H., Liu, Y., Liu, J., ... & Lee, S. T. (2010). Water-soluble fluorescent carbon quantum dots and photocatalyst design. *Angewandte Chemie International Edition*, *49*(26), 4430–4434.

Li, R., Zhang, F., Wang, D., Yang, J., Li, M., Zhu, J., ... & Li, C. (2013). Spatial separation of photogenerated electrons and holes among {010} and {110} crystal facets of $BiVO_4$. *Nature Communications*, *4*(1), 1432.

Li, W. W., Yu, H. Q., & He, Z. (2014). Towards sustainable wastewater treatment by using microbial fuel cells-centered technologies. *Energy & Environmental Science*, *7*(3), 911–924.

Li, Y., Wang, H., Xie, L., Liang, Y., Hong, G., & Dai, H. (2011). MoS_2 nanoparticles grown on graphene: an advanced catalyst for the hydrogen evolution reaction. *Journal of the American Chemical Society*, *133*(19), 7296–7299.

Linic, S., Christopher, P., & Ingram, D. B. (2011). Plasmonic-metal nanostructures for efficient conversion of solar to chemical energy. *Nature Materials*, *10*(12), 911–921.

Linsebigler, A. L., Lu, G., & Yates, J. T., Jr. (1995). Photocatalysis on TiO_2 surfaces: principles, mechanisms, and selected results. *Chemical Reviews*, *95*(3), 735–758.

Liu, G., Niu, P., Sun, C., Smith, S. C., Chen, Z., Lu, G. Q., & Cheng, H. M. (2010). Unique electronic structure induced high photoreactivity of sulfur-doped graphitic C_3N_4. *Journal of the American Chemical Society*, *132*(33), 11642–11648.

Loeb, S. K., Alvarez, P. J., Brame, J. A., Cates, E. L., Choi, W., Crittenden, J., ... & Kim, J. H. (2018). The technology horizon for photocatalytic water treatment: sunrise or sunset? *Environmental Science & Technology*, *53*(6), 2937–2947.

Loos, R., Carvalho, R., António, D. C., Comero, S., Locoro, G., Tavazzi, S., ... & Gawlik, B. M. (2013). EU-wide monitoring survey on emerging polar organic contaminants in wastewater treatment plant effluents. *Water Research*, *47*(17), 6475–6487.

Mintcheva, N., Aljulaih, A. A., Wunderlich, W., Kulinich, S. A., & Iwamori, S. (2018). Laser-ablated ZnO nanoparticles and their photocatalytic activity toward organic pollutants. *Materials*, *11*(7), 1127.

Moattari, R. M., & Mahinroosta, M. (2025). Magnetic hematite (α-Fe_2O_3) photocatalyst in wastewater treatment. In *Metal Oxide Based Nanophotocatalyst for Wastewater Purification* (pp. 193–230). Springer Nature Singapore.

Mondal, B., & Saha, S. K. (2012). Surfactant-assisted hydrothermal synthesis of CdS nanotips: optical and magnetic properties. *Journal of Nanoparticle Research*, *14*(8), 1049.

Ndiaye, D., & Akill, A. (2025). A critical review on g-C_3N_4 for environmental remediation: synthesis, properties, and pollutant photodegradation. *Rendiconti Lincei. Scienze Fisiche e Naturali*, 1–25.

Nosaka, Y., & Nosaka, A. Y. (2017). Generation and detection of reactive oxygen species in photocatalysis. *Chemical Reviews*, *117*(17), 11302–11336.

Nowotny, M. K., Sheppard, L. R., Bak, T., & Nowotny, J. (2008). Defect chemistry of titanium dioxide. Application of defect engineering in processing of TiO_2-based

photocatalysts. *The Journal of Physical Chemistry C*, *112*(14), 5275–5300.

Pan, X., Yang, M. Q., Fu, X., Zhang, N., & Xu, Y. J. (2013). Defective TiO_2 with oxygen vacancies: synthesis, properties and photocatalytic applications. *Nanoscale*, *5*(9), 3601–3614.

Pelaez, M., Nolan, N. T., Pillai, S. C., Seery, M. K., Falaras, P., Kontos, A. G., ... & Dionysiou, D. D. (2012). A review on the visible light active titanium dioxide photocatalysts for environmental applications. *Applied Catalysis B: Environmental*, *125*, 331–349.

Petrie, B., Barden, R., & Kasprzyk-Hordern, B. (2015). A review on emerging contaminants in wastewaters and the environment: current knowledge, understudied areas and recommendations for future monitoring. *Water Research*, *72*, 3–27.

Pignatello, J. J., Oliveros, E., & MacKay, A. (2006). Advanced oxidation processes for organic contaminant destruction based on the Fenton reaction and related chemistry. *Critical Reviews in Environmental Science and Technology*, *36*(1), 1–84.

Reddy, J. K., Suresh, G., Hymavathi, C. H., Kumari, V. D., & Subrahmanyam, M. (2009). Ce(III) species supported zeolites as novel photocatalysts for hydrogen production from water. *Catalysis Today*, *141*(1–2), 89–93.

Rincon, A. G., & Pulgarin, C. (2004). Effect of pH, inorganic ions, organic matter and H_2O_2 on E. coli K12 photocatalytic inactivation by TiO_2: implications in solar water disinfection. *Applied Catalysis B: Environmental*, *51*(4), 283–302.

Sakthivel, S., Neppolian, B., Shankar, M. V., Arabindoo, B., Palanichamy, M., & Murugesan, V. (2003). Solar photocatalytic degradation of azo dye: comparison of photocatalytic efficiency of ZnO and TiO_2. *Solar Energy Materials and Solar Cells*, *77*(1), 65–82.

Sapkal, R. T., Shinde, S. S., Mahadik, M. A., Mohite, V. S., Waghmode, T. R., Govindwar, S. P., ... & Bhosale, C. H. (2012). Photoelectrocatalytic decolorization and degradation of textile effluent using ZnO thin films. *Journal of Photochemistry and Photobiology B: Biology*, *114*, 102–107.

Sathish, M., Viswanathan, B., & Viswanath, R. P. (2007). Characterization and photocatalytic activity of N-doped TiO_2 prepared by thermal decomposition of Ti–melamine complex. *Applied Catalysis B: Environmental*, *74*(3–4), 307–312.

Schneider, J., Matsuoka, M., Takeuchi, M., Zhang, J., Horiuchi, Y., Anpo, M., & Bahnemann, D. W. (2014). Understanding TiO_2 photocatalysis: mechanisms and materials. *Chemical Reviews*, *114*(19), 9919–9986.

Schwarzenbach, R. P., Egli, T., Hofstetter, T. B., Von Gunten, U., & Wehrli, B. (2010). Global water pollution and human health. *Annual Review of Environment and Resources*, *35*, 109–136.

Spasiano, D., Marotta, R., Malato, S., Fernandez-Ibanez, P., & Di Somma, I. (2015). Solar photocatalysis: materials, reactors, some commercial, and pre-industrialized applications. A comprehensive approach. *Applied Catalysis B: Environmental*, *170*, 90–123.

Subramanian, V., Wolf, E. E., & Kamat, P. V. (2004). Catalysis with TiO_2/gold nanocomposites. Effect of metal particle size on the Fermi level equilibration. *Journal of the American Chemical Society*, *126*(15), 4943–4950.

Tran, T. H., & Nguyen, V. T. (2014). Copper oxide nanomaterials prepared by solution methods, some properties, and potential applications: a brief review. *International Scholarly Research Notices*, *2014*(1), 856592.

Turchi, C. S., & Ollis, D. F. (1990). Photocatalytic degradation of organic water contaminants: mechanisms involving hydroxyl radical attack. *Journal of Catalysis*, *122*(1), 178–192.

Valadez-Renteria, E., Perez-Gonzalez, R., Gomez-Solis, C., Díaz-Torres, L. A., Encinas, A., Oliva, J., & Rodriguez-Gonzalez, V. (2023). A novel and stretchable carbon-nanotube/Ni@TiO_2:W photocatalytic composite for the complete removal of diclofenac drug from drinking water. *Journal of Environmental Sciences*, *126*, 575–589.

Walser, T., Demou, E., Lang, D. J., & Hellweg, S. (2011). Prospective environmental life cycle assessment of nanosilver T-shirts. *Environmental Science & Technology*, *45*(10), 4570–4578.

Wang, H., Zhang, L., Chen, Z., Hu, J., Li, S., Wang, Z., ... & Wang, X. (2014). Semiconductor heterojunction photocatalysts: design, construction, and photocatalytic performances. *Chemical Society Reviews*, *43*(15), 5234–5244.

Wang, S., & Wang, X. (2015). Multifunctional metal–organic frameworks for photocatalysis. *Small*, *11*(26), 3097–3112.

Wang, X., Maeda, K., Thomas, A., Takanabe, K., Xin, G., Carlsson, J. M., ... & Antonietti, M. (2009). A metal-free polymeric photocatalyst for hydrogen production from water under visible light. *Nature Materials*, *8*(1), 76–80.

Woan, K., Pyrgiotakis, G., & Sigmund, W. (2009). Photocatalytic carbon-nanotube–TiO_2 composites. *Advanced Materials*, *21*(21), 2233–2239.

Xu, D., Shi, W., Song, C., Chen, M., Yang, S., Fan, W., & Chen, B. (2016). In-situ synthesis and enhanced photocatalytic activity of visible-light-driven plasmonic Ag/AgCl/$NaTaO_3$ nanocubes photocatalysts. *Applied Catalysis B: Environmental*, *191*, 228–234.

Yan, H., Chen, Y., & Xu, S. (2012). Synthesis of graphitic carbon nitride by directly heating sulfuric acid treated melamine for enhanced photocatalytic H_2 production from water under visible light. *International Journal of Hydrogen Energy*, *37*(1), 125–133.

Zhang, H., Lv, X., Li, Y., Wang, Y., & Li, J. (2010). P25-graphene composite as a high performance photocatalyst. *ACS Nano*, *4*(1), 380–386.

Zhang, J., Yu, J., Zhang, Y., Li, Q., & Gong, J. R. (2011). Visible light photocatalytic H_2-production activity of CuS/ZnS porous nanosheets based on photoinduced interfacial charge transfer. *Nano Letters*, *11*(11), 4774–4779.

Zhang, J., Zhou, P., Liu, J., & Yu, J. (2014). New understanding of the difference of photocatalytic activity among anatase, rutile and brookite TiO_2. *Physical Chemistry Chemical Physics*, *16*(38), 20382–20386.

Zhang, L., Wang, W., Zhou, L., & Xu, H. (2007). Bi_2WO_6 nano- and microstructures: shape control and associated visible-light-driven photocatalytic activities. *Small*, *3*(9), 1618–1625.

Zhang, Z., Wang, C. C., Zakaria, R., & Ying, J. Y. (1998). Role of particle size in nanocrystalline TiO_2-based photocatalysts. *The Journal of Physical Chemistry B*, *102*(52), 10871–10878.

Zhou, P., Yu, J., & Jaroniec, M. (2014). All-solid-state Z-scheme photocatalytic systems. *Advanced Materials*, *26*(29), 4920–4935.

Zhu, J., Deng, Z., Chen, F., Zhang, J., Chen, H., Anpo, M., ... & Zhang, L. (2006). Hydrothermal doping method for preparation of Cr^{3+}-TiO_2 photocatalysts with concentration gradient distribution of Cr^{3+}. *Applied Catalysis B: Environmental*, *62*(3–4), 329–335.

Zukalová, M., Zukal, A., Kavan, L., Nazeeruddin, M. K., Liska, P., & Grätzel, M. (2005). Organized mesoporous TiO_2 films exhibiting greatly enhanced performance in dye-sensitized solar cells. *Nano Letters*, *5*(9), 1789–1792.